SCIENCE CHINA
Information Sciences

August 2019, Vol. 62 080305:1–080305:19
https://doi.org/10.1007/s11432-018-9858-2

• RESEARCH PAPER •
Special Focus on B5G Wireless Communication Networks

Exploring multiamplitude voltage modulation to improve spectrum efficiency in low-complexity visible-light communication

Xiangyu LIU[1], Xuetao WEI[2], Lei GUO[3*] & Yejun LIU[3]

[1]*School of Computer Science and Engineering, Northeastern University, Shenyang* 110819*, China;*
[2]*School of Information Technology, University of Cincinnati, Cincinnati* 45221*, USA;*
[3]*School of Communication and Information Engineering, Chongqing University of Posts and Telecommunications, Chongqing* 400044*, China*

Received 21 June 2018/Revised 24 December 2018/Accepted 8 April 2019/Published online 11 July 2019

Abstract Owing to the recent advancements in the Internet of Things (IoT), an increasing number of IoT devices have led to frequency crowding in wireless networks. The low-complexity visible light communication (VLC) system is a promising solution for indoor frequency-crowded wireless networks owing to the ubiquity of light-emitting diodes (LEDs) and readily deployable, low-cost modulation methods. However, due to the inherent limitations of LED materials and growth of data from IoT applications, low-complexity VLC systems can barely boost the data throughput without adding complex modulations and circuits. This study aims to design and implement a spectrum-efficient, low-complexity VLC system to improve data throughput with very little cost to support indoor IoT applications. This system uses multiamplitude voltage to transmit multiple bit streams simultaneously, making it a novel system. However, it is not trivial to achieve this goal as the varying voltage can cause the LEDs to flicker. Therefore, we further propose a voltage-to-current amplifier circuit, which effectively mitigates the effects of changes in the LED's brightness upon human eyes. Finally, we evaluate the system under different speeds, distances, and angles. Extensive experiments demonstrate promising results from the viewpoint of spectrum efficiency, throughput, bit-error rate, and user perception.

Keywords visible light communication, amplitude modulation, spectral efficiency

Citation Liu X Y, Wei X T, Guo L, et al. Exploring multiamplitude voltage modulation to improve spectrum efficiency in low-complexity visible-light communication. Sci China Inf Sci, 2019, 62(8): 080305, https://doi.org/10.1007/s11432-018-9858-2

1 Introduction

5G networks have been standardized and will be widely deployed in 2020. Beyond 5G (B5G) networks have become hotspots because they cover global networks (including sky, land and ocean). B5G network utilizes enormous bandwidth resources to meet communication needs, including millimeter wave communication, visible light communication, and so on. Visible-light communication (VLC) is a promising technology for enabling various applications owing to the ubiquity of light-emitting diodes (LEDs) around us [1]. With the recent advancements in the Internet of Things (IoT), light-based communication serves as an important and alternative communication scheme for IoT applications, including visible-light sensing [2, 3], consumer electronics [4], Narrowband IoT (NB-IoT) [5], and open web of things [6]. The characteristics of such devices are low-complexity, low-speed, and short communication distances. For

* Corresponding author (email: guolei@cqupt.edu.cn)

© Science China Press and Springer-Verlag GmbH Germany, part of Springer Nature 2019

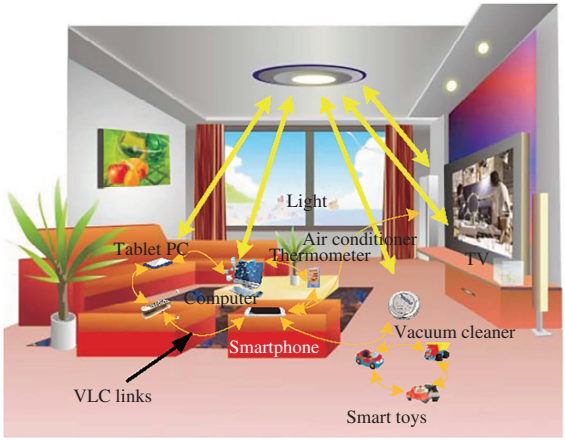

Figure 1 (Color online) Low-complexity visible-light communication (VLC) systems for smart illumination and consumer devices, e.g., smart toys, smart glasses, and other IoT devices.

example, light-based communication can be used for home-entertainment scenarios, such as smart toys that communicate with each other [7]. Furthermore, it offers a superior security performance to radio frequency (RF) alternatives, which can be used to replace RF-based wireless-authentication applications such as vending machines. The readily deployable, low-cost modulation unit could easily turn LEDs into low-complexity LED-based VLC systems for indoor IoT applications, as shown in Figure 1.

The bandwidth LED is relatively small, i.e., in the range of 1–3 MHz, due to the limitations of LED materials, which is not ideal for the growth of data from these low-complexity VLC systems [8–10]. When the size of communication networks increases, all nodes collectively occupy a limited bandwidth. Therefore, spectrum efficiency should be improved to accommodate more devices even at low speeds. Although there are high-precision, high-performance, and computationally intensive chips to support advanced modulation methods, such as orthogonal-frequency-division multiplexing (OFDM), code-shift keying (CSK), discrete multi-tone, and space modulation (SM) [9, 11–13], the deployment cost is high, which may prohibit the widespread promotion of VLC systems. Furthermore, LEDs are noncoherent light sources [14]. Frequency-modulation and phase-modulation schemes, such as frequency-shift keying (FSK) and phase-shift keying (PSK) [15–17], are not convenient as extra frequency- and phase-compensation circuits must be designed to drive LEDs. Therefore, an approach that improves spectrum efficiency should be proposed to boost the throughput for the low-complexity VLC system without adding computationally intensive chips or complex circuits. To achieve this, herein, multiamplitude voltage modulation is used to improve spectrum efficiency. Note that, though the multiamplitude-modulation approach has been widely used in wireless and optical fiber communications [18, 19], it is challenging for LEDs in VLC systems as the varied voltage may cause the severe flicker problem of LEDs for human eyes, making VLC systems impractical for indoor IoT applications. Previous studies [20, 21] mainly focused on adding complex-drive circuits to avoid the LED's flicker, and these are not suitable for the ubiquitous deployment of low-complexity VLC systems.

Herein, we design and implement a spectrum-efficient, low-complexity VLC system enabled by an efficient multiple-amplitude pulse-position-modulation (MAPPM) scheme to improve spectrum efficiency and a voltage-to-current-amplifier circuit to avoid the LED's flicker. Traditionally, the widely-used modulation method for low-complexity VLC devices is on-off keying (OOK). This uses the "dark" and "bright" settings of an LED to represent the bits "1" and "0", respectively. Note that bright means that light is emitted and dark means no light is emitted) [6, 7]. However, a sequence of "0s", e.g., "000", will turn off the LED for a period that could impact user perception on the light, e.g., flicking lights. Therefore, a prior study proposed two-pulse-position modulation (2-PPM) using "1(bright)0(dark)" and "0(dark)1(bright)" to represent the bits "1" and "0", respectively, preventing the LED from flicker [22]. However, we can observe that this additional bit caused inefficient spectrum usage; one bit's information is represented by two symbols rather than one.

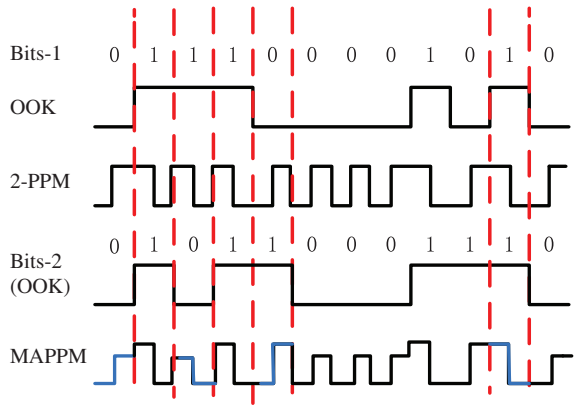

Figure 2 (Color online) The principles of our multiple-amplitude pulse-position-modulation (MAPPM) scheme, as compared with two readily deployable modulation methods, such as on-off keying (OOK) and 2-PPM, in low-complexity VLC systems. Our MAPPM scheme enables two bit streams to transmit simultaneously by modulating the signal with multiple states (where the blue line represents different states).

Herein, we introduce the multiamplitude voltage to increase every bit's information to transmit two bit streams simultaneously. Due to certain hardware limitations of current off-the-shelf low-complexity devices, we focus only on two bit streams to demonstrate the feasibility of our proposed approach, and will investigate the case of more-bit streams in future work. Herein, every bit's information comprises "dark, softly bright, bright" rather than "dark, bright". As shown in Figure 2, we reduce the voltage of "bright" to a certain value as "softly bright". The "bright" and "softly bright" represent the bits "1" and "0,", respectively, in the second bit stream (Bits-2). The "dark, bright" or "dark, softly bright" represents the bit "0" in the first bit stream (Bits-1), The "bright, dark" or "softly bright, dark" represent the bit "1" in the first stream (Bits-1). Furthermore, it is challenging to define the voltage value of "softly bright" to ensure that the receiver's bit-error rate (BER) is as low as possible. Meanwhile, human eyes cannot perceive the LED's flicker and change in brightness. Thus, we further design and implement a simple structured voltage-to-current-conversion amplifier circuit to prevent human eyes from perceiving the LED's flicker and mitigate the impact of the change in brightness. In the end, we prototype the proposed VLC system using off-the-shelf and low-complexity devices. We evaluate the effectiveness of the proposed system based on the system's spectrum efficiency and BER via thorough experiments, e.g., different angles, speeds, and distances. To the best of our knowledge, the proposed study is the first to explore the effect of multiamplitude voltage modulation to improve the spectrum efficiency and boost the throughput in low-complexity VLC systems.

Our detailed contributions are summarized as follows.

(1) We propose a novel spectrum-efficient modulation scheme called MAPPM for low-complexity VLC systems. This scheme takes advantage of multiamplitude voltage to transmit two bit streams simultaneously to double the spectrum efficiency. It splits the high-level voltage of the first bit stream into two minor-difference voltages to represent the second bit stream's high and low levels, respectively. In the transmitter, we design and implement a sequence header by only adding two square waves of different periods to synchronize the system and enhance the receiver's correct sampling. In the receiver, microcontroller averages two slightly different voltages as the threshold to decompose the synthetic bit stream.

(2) We design and implement a voltage-to-current amplifier circuit, which aims to avoid human perception of the LED's flicker and to mitigate the effects of change in brightness. It comprises two parts, a voltage-to-voltage amplifier circuit and a voltage-to-current amplifier circuit based on one transistor. The former is used to decrease the output impedance of transmitter pins, and then to provide an adaptive-input voltage for the second part. The latter is used to change the current through the LED subtly such that the transmitter will not drastically change the brightness.

(3) We build a prototype using off-the-shelf and low-cost devices and evaluate our proposed system

by conducting experiments. We extensively tested the BER and spectrum efficiency at different speeds, distances, and angles. We also conducted a study of the user perception of the LED's brightness and the flicker in both daytime and nighttime. Our evaluation results showed that our proposed system achieves promising results.

2 Related work

Most previous studies have not considered multiamplitude voltage modulation to improve spectrum efficiency in the low-complexity VLC system. They have also not considered the use of off-the-shelf and low-cost devices to realize such modulation. Below, we discuss prior work on VLC-modulation schemes and general-VLC applications.

2.1 The VLC modulation

VLC uses the visible-light band as the information carrier without optical fiber or other cable channels to transmit signals through the air [23]. The biggest advantage is to mitigate resource contention in the wireless spectrum and to reduce interference between wireless channels. Owing to the ubiquitous presence of LEDs in practice, visible-light communication using LEDs with an instantaneous on/off feature has been extensively studied to support numerous applications. For example, it could be integrated with WiFi, cellular networks (3G, 4G, and even 5G), and other communications technologies in the domains of smart cities, aviation, navigation, subway, high-speed rail, and indoor-navigation applications, among others; thereby, further promoting the development of the Internet of Everything [24–26]. The most significant difference between wireless communication and VLC is that the bit stream cannot be modulated in phase with the light signal [27,28]. This means that modulation techniques are based on intensity modulation/direct detection (IM/DD). IEEE 802.15.7 discussed four types of modulation schemes: (1) OOK, which is the simplest form of the amplitude-shift-keying modulation that represents digital signals as the presence or absence of a carrier wave with the presence of a carrier wave representing '1' and its absence representing '0' [22]; (2) pulse modulation, which has been used widely in optical-communication systems, generates pulses of equal amplitude at a rate controlled by the modulated signal's amplitude; its major advantage is high power efficiency using pulse modulations, such as PPM [29], PWM [30], VPPM [31]; (3) orthogonal-frequency-division modulation (OFDM) is developed by multi-carrier modulation; it is one way to realize a multi-carrier-transmission scheme. Its modulation and demodulation are realized based on the inverse fast Fourier transform and fast Fourier transformation, respectively. The major difference between VLC- and wireless-based OFDM is that VLC-based OFDM cannot achieve bipolar signal transmission, and the receiver can only detect signals by IM/DD [9]; and (4) color-shift modulation (CSK), which is a novel modulation method for VLC systems with RGB-LEDs that transmits signals through the color property of a multi-color light source. For the receiver, the spectral-response characteristics of the photodetector are used to generate different voltages, thereby demodulating signals [11]. The first two modulation schemes are widely used in low-complexity systems, since they are readily deployable. The others, i.e., wavelength-division multiplexing (WDM) [32] and spatial modulation (SM) [13], are mainly used in high-speed and high-performance systems equipped with high-precision and computationally intensive chips. Zhang et al. [33] proposed energy-efficient space-time modulation for peak-limited MISO-broadcast VLC systems by cooperatively managing the nonnegative multiuser interference. In addition, they [34] proposed an energy-efficient time-collaborative modulation constellation by minimizing the total optical power subject to a fixed minimum Euclidean distance without channel-state information at the transmitter. Chau et al. [35] proposed a new MIMO VLC-receiver architecture capable of dynamically adjusting the optical channel using a spatial light modulator. However, they focused on energy efficiency, and furthermore, either the transmitter or the receiver had to be of increased complexity as either multiple LEDs in the transmitter or multiple photodetectors in the receiver are required to improve spectrum efficiency. Gancraz et al. [36] proposed an approach toward dimming and data transmission through the variation of codeword weights in overlapping pulse-position modulation. Although it can

improve spectrum efficiency, they did not consider the LEDs' flicker problem. When the codeword weight is small, the LEDs' flicker will appear because the interval between sample codewords is too large.

Herein, we focus on the readily deployable modulation schemes used in low-complexity VLC systems, which are applied in many different areas, e.g., visible-light sensing, smart toys, smart glasses and other IoT devices [6, 7, 37, 38].

2.2 VLC applications

LEDs are semiconductor electronic devices that are used for transforming electrical energy into light [39]. LEDs are based on semiconductor chips, which are mainly composed of P- and N-type semiconductors. Recently, LEDs have undergone high-speed development, as their brightness has been enhanced by 20 times and their cost reduced by 99% every year. The impact of LED technology has been extended to the global science and technology, economy, life, and other fields. In comparison with incandescent, energy-saving lamps, and other light sources, LEDs have the advantages of higher modulation bandwidths, higher efficiency, longer life and higher sensitivity. LED energy consumption is far lower than other light sources, whereas the brightness efficiency is higher. This meets the "green, low-consumption" concept [40–44]. In [45–47], the authors studied indoor-positioning technology under the condition of LEDs with accelerometers, trilateration algorithms, and channel hopping. They found that the VLC can achieve high-accuracy localization than the existing indoor localization systems such as, WiFi based. Arai et al. [48] proposed a network model and built an experimental platform for vehicular-communication systems, providing a strong basic framework for subsequent outdoor VLC. Wang et al. [49] proposed test platforms using BeagleBone Black, which aimed to promote the development of VLC in various fields. Schmid et al. [7, 38] proposed LED-LED communications and LED-LED networks, which changed the development of receiving ends and up-links. Li et al. [50] proposed screen-camera communications under any scene, which could simultaneously transmit images and tests at the same time. Hao et al. [51] proposed COBRA, an innovation arising from using two-dimensional code in VLC fields. Tian et al. [6,37] proposed darkVLC, which aimed at achieving VLC in dark environments. Anran et al. [52] also proposed screen-camera communications, which leveraged the temporal flick-fusion property of human-vision systems and fast frame rate of a modern display. Schmid et al. [4] proposed the use of consumer LED bulbs for low-cost and low-complexity VLC systems. The Internet protocol connectivity based on networked light bulbs and sensing human activities was explored to develop an indoor VLC network in [53–58].

However, the problem of spectrum efficiency has been ignored by previous study, greatly limiting the development of low-complexity VLC systems and their applications.

3 Design

In this section, we will present the design of our MAPPM scheme in detail.

3.1 Concept

Most LEDs are still noncoherent light sources, and VLC commonly uses the intensity modulation/direct detection (IM/DD) methods for communication. Frequency and phase-modulation methods require additional compensation circuits or high-performance chips, such as FSK, PSK, and OFDM [9, 17]. They are not suitable for low-complexity VLC devices. Therefore, OOK and 2-PPM methods are used widely in low-complexity VLC systems [22].

When we use OOK modulation, the long "0" in the bit stream, which means that the LED always remains "dark," will cause the flicker. The 2-PPM method is proposed to avoid human eyes perceiving the flicker during communication, as shown in Table 1. It uses "(bright, dark)" to represent "0" and "(dark, bright)" to represent "1". Note that "bright" means light is emitted and "dark" means no light. In this manner, LED flicker can be eliminated. However, an additional symbol, which is used to eliminate the flicker, causes inefficient usage of LED bandwidth. Herein, we introduce a MAPPM scheme that takes

Table 1 2-PPM modulation scheme[a)]

Bit	(first symbol, second symbol)
0	(bright, dark)
1	(dark, bright)

a) Bright means that light is emitted; dark means no light.

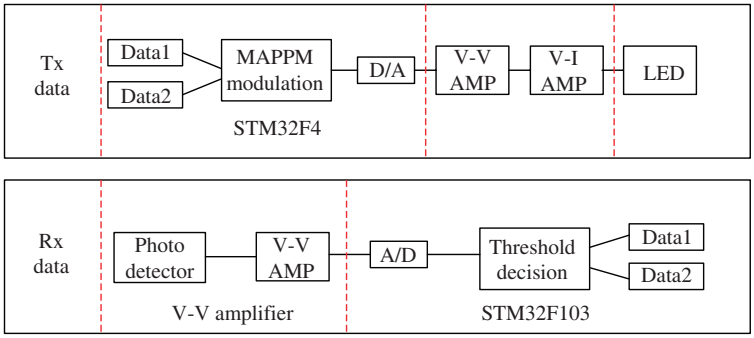

Figure 3 (Color online) The system architecture. The second bit stream is embedded in the first by the MAPPM scheme. The synthetic bit stream is transmitted into the V-I circuit so that human eyes cannot perceive the flicker. Then, it passes through the photodetector and amplifier to produce A/D conversion and threshold decision.

advantage of multiamplitude voltage to transmit two bit streams simultaneously, thereby improving the spectrum efficiency significantly.

Figure 3 shows the proposed VLC architecture comprising three modules, including a MAPPM scheme, voltage-to-current conversion circuits, and adaptive threshold. First, we increase every bit's information by multiamplitude voltages. When the second bit stream comes, we synthesize the two bit streams into a new bit stream, which is made up of three states: "dark", "softly bright," and "bright". The new bit stream is further assigned to the digital-to-analog (D/A) converter module. Then, the bit stream is transmitted by voltage-to-voltage operational amplifier and voltage-to-current amplifier circuits, which aim to mitigate the effects of flicker and brightness.

At the receiver, the transmitted light is concentrated onto the photodetector. Then, the receiver extracts the synthetic bit stream from the photodetector using a voltage-to-voltage amplifier circuit and an A/D-conversion module. Two bit streams can be easily demodulated with two timers and one adaptive threshold. These demodulation bits can be correctly identified according to corresponding voltages. Voltages are related to distances, speeds, and angles, among others.

3.2 Modulation

We illustrate the principle of MAPPM in Figure 2. There are two bit streams, Bits-1 and 2. We embed Bits-2 into Bits-1 using the "OOK+PPM" method. For the synthetic bit stream, there are four cases: "0, 0", "0, 1", "1, 0", and "1, 1". Note that these are ordered. The first position refers to Bits-1, the second to Bits-2. We use four different light-intensity levels to represent these four cases: "dark, softly bright", "dark, bright", "softly bright, dark", and "bright, dark". The final synthetic result is the blue-line case, as shown in Figure 2. The PPM originally uses two symbols to represent one bit. However, we use two symbols to represent two bit streams under the MAPPM scheme. One is Bits-1, another is Bits-2. Thus, the spectrum efficiency doubles. In our test, we find that, when we set the amplitude difference between "softly bright" and "bright" at 40 mv and change of current passing through the LEDs is 100 μA, human eyes cannot perceive flicker. This is described in Subsection 5.1.

3.3 Flicker and brightness

Due to the use of multiple voltage amplitudes, we have to ensure that our MAPPM scheme does not generate flicker or LED-brightness changes.

Flicker. First, we analyze the influence of flicker, which is defined as the fluctuation of the brightness of light that can cause noticeable physiological changes in human eyes [59]. We strive to mitigate flicker that may be caused by modulation of light sources for communication. The maximum flickering time period (MFTP) is defined as the maximum time period over which the light intensity may change but the resulting flicker is not perceptible by human eyes [60]. To eliminate the flicker, we must avoid changes in brightness over periods longer than the MFTP. As long as the flicker frequency is fast enough, human eyes will not perceive the flicker. For our "bright, softly bright, dark" combinations, if the transmitted frequency is adjusted properly, the problem of flicker can be solved.

Brightness. The second problem is the brightness. This is related to duty ratio and light intensity [59]. In [6], the authors proposed darkVLC, which means that the VLC can transmit data in dark. The principle is to make the brightness of the duty ratio extremely small so that human eyes cannot perceive this pulse light. In [50], the authors proposed screen communications under any scene, transmitting extra data by changing the gray level of the α-channel on screen. Human eyes could not perceive the change of the gray level. The principle is to change the light intensity. Therefore, we conclude that we can change the brightness of the LED subtly by changing the light intensity and duty ratio while ensuring that human eyes cannot perceive the variation of brightness.

Note that human eyes are complicated optical systems, capable of generating various perceptions in all kinds of situations, e.g., different distances, angles, and ambient light. Therefore, we must change the light intensity to be as small as possible and appropriately decrease the duty ratio so that human eyes cannot perceive flicker or change in brightness. Herein, we generate tiny changes in light intensity using voltage-to-current circuits and change the duty ratio by setting the appropriate transmitter speed. We introduce our voltage-to-current circuits in Section 4.

In addition, we considered the use of different frequencies or signal phases to represent two different bit streams, which can effectively avoid changes in brightness and flicker problems. This method is similar to the QPSK scheme [61]. However, we find that there is a serious problem with using LEDs in practice: the LED is an incoherent light source. The frequency and phase of the emitted light change irregularly, which means that we have to rely upon sophisticated equipment and complex circuits for frequency and phase compensation. This is not our goal, as it significantly limits the applicability of low-complexity VLC systems in the real world.

3.4 Demodulation

For the receiver, we can demodulate the synthetic bit stream into two bit streams by setting the proper threshold. We assume that the final synthetic bit stream is the waveform at the bottom of Figure 2. We only need to set a timer to conduct the A/D conversion to sample the data at the appropriate time. Then, we compare the sampled data with the threshold. Finally, we obtain two bit streams from the synthetic bit stream. For the threshold value, the receiver samples a set of data. Then, we use the average value of "bright" and "softly bright" as it.

3.5 Synchronization

During the receiving processes, we need to know when the second bit stream arrives and ends. Therefore, we add a sequence header in front of the bit stream. The sequence header acts as follows: (1) it determines the arrival time of the second bit stream and (2) it provides the clock signal for the receiver-sampling data. Specific processes are shown in Figure 4. We introduce a 150 μs low level at the initial end. Then, we add a 200 μs high level and 150 μs low level. Finally, we transmit the bit stream after waiting for a 100 μs high-level duration.

For the receiver, when the Timer1's capture time is less than 200 or 340 μs, we think that the second bit stream arrives. Then, Timer2 opens the count function in the next rising edge. Next, we sample the data when Timer2 interrupts. We set Timer2's count time to 300 μs. The purpose of waiting for 100 μs after the rising edge is to decrease the influence of computation and rising and falling edges. Final, if

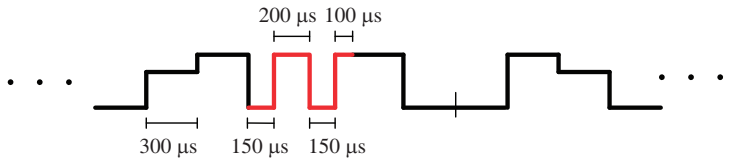

Figure 4 (Color online) The architecture of the sequence header. We set the same duration of 600 μs for both one bit and sequence header. Then, we set different lengths of time in the sequence header to avoid the flicker and synchronize the receiver. The duration time of the header sequence varies with the duration time of one bit, i.e., the duration time varies with different speeds.

the "softly bright" level does not appear for a long time, the second bit stream is concluded to be over. When the next bit stream comes, we add the sequence header again.

For the transmitter, although the duty cycle of 200 and 100 μs can cause changes in brightness, it can be ignored when a long-sequence bit stream arrives. If the second bit stream is transmitted in a cycle, we can change 200 to 340 μs, as long as the receiver is able to capture it accurately.

4 Prototype

In this section, we present our system prototype for the MAPPM scheme. Transmitter and receiver circuits are important to meet the nonflicker and brightness requirements. Next, we briefly describe our prototype.

4.1 Transmitter

We used STM32F407ZGT6 microcontroller unit and an LED as the system transmitter. STM32 is chosen as our microcontroller because it is cheap and popular on the market. Moreover, its dominant frequency is 184 MHz and it has the built-in 12-bit successive-approximation-type D/A converter, which produces a 0.0001 V change. It is also more convenient than low-performance microcontrollers, such as, 80C51, Arduino, which need an additional D/A-conversion module.

To meet the nonflicker and brightness requirements, we need to design an LED-drive circuit. The reasons are as follows: (1) STM32's D/A-conversion module pin-output voltage is around 3.3 V, and the output impedance is higher than the LED's internal resistance. If we directly connect the pin to the LED, the pin-output impedance will yield a higher voltage than the LED so that the LED cannot obtain sufficient voltage (Final, voltage will transform current.) to drive the LED lighting. (2) We can lower pin-output impedance by adding a voltage follower to achieve the required brightness. However, the LED is derived from a constant current source, and a small change in the voltage will have a dramatic change in the current, as can be observed through Figure 5. Although we can slightly change the voltage of the LED, a dramatic change in the current will obviously change the brightness so that human eyes can perceive the variety of brightness and flicker.

Thus, we design the transmitter-drive circuit, as shown in Figure 6. The circuit comprises two parts. The first is a voltage-to-voltage operational amplifier circuit, whose closed-loop gain is 2. Its purpose is to provide a suitable voltage for the second part. It is also the buffer to decrease the microcontroller pin-output impedance. The second part is a voltage-to-current-converter amplifier circuit, which is made up of a transistor and operational amplifier, with current-series depth-negative feedback. The V_+ of the OPA07CPA operational amplifier is the signal-input port. The emitter current $I_{\rm e}$ of the transistor acts upon resistance R5 and LED internal resistance. By the amplification principle of the transistor, we know that

$$V_- = I_e \times (R_5 + R_{\text{led-r}}), \tag{1}$$

$$I_e = \beta \times I_b. \tag{2}$$

By operational amplifier virtual short and virtual open, we can see that

$$V_+ = V_-, \tag{3}$$

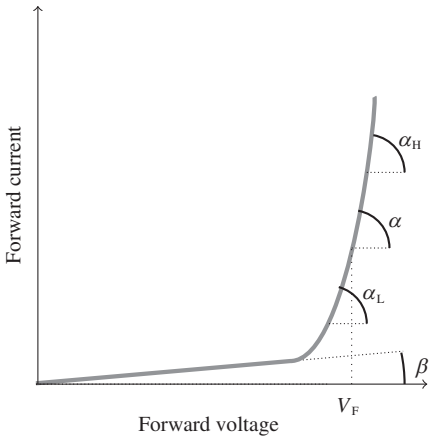

Figure 5 LED I-V characteristic and its slopes. The forward current is slowly growing when the LED does not reach the turn-on voltage, the slope $\beta = \mathrm{d}V/\mathrm{d}I$. After reaching the turn-on voltage, the forward current has a sharp rise, and the slope becomes α, which is clearly increasing.

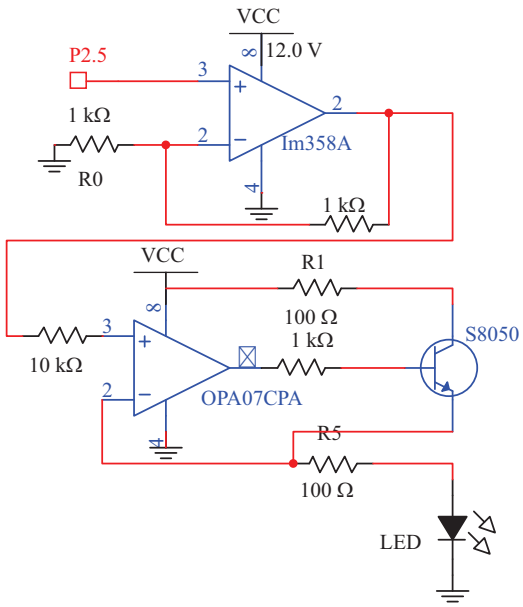

Figure 6 (Color online) The circuit diagram of V-I conversion. It consists of two parts. The first part is the V-V amplifier circuit. The second part is the V-I amplifier circuit based upon the transistor. The current is controlled by transistors and resistors.

$$I_o = I_e \approx V_+/(R_5 + R_{\text{led-r}}), \tag{4}$$

where I_b is the base current and I_o is the current through the LED. By adjusting the resistor R_5, the circuit can generate a suitable current for the LED. The resistor R_1 serves to adjust the quiescent operation point of the transistor to produce the appropriate negative feedback. The simplified equation is

$$I_l \approx \frac{P_{2.5} \times 2}{R_5}. \tag{5}$$

We assume the resistance R_5 is 100 Ω. Using (5), we find that the change of 0.1 V in the pin will produce a change of 0.002 A. Furthermore, if the resistor R_5 is 1000 Ω, the change in current will be only 0.0002 A. When R_5 is large enough, $R_{\text{led - r}}$ becomes insignificant and is ignored. We are able to control the current through R_5; thus, this method is much better than directly controlling the change of voltage.

4.2 Receiver

We use STM32F103C8 microcontroller unit and a photodetector as the system receiver. STM32F103C8 has a built-in 12-bit successive-approximation-type A/D converter, meaning that it is more convenient than a microcontroller with an extra A/D-converter module. Meanwhile, the built-in filter can also help us to eliminate disturbances from the light noise.

For the photodetector, we choose SD5421. It comprises PIN photodiode and is suitable for operations in light noise environments. This detector is selected for the following reasons. For low-complexity VLC devices, this photodetector offers a high response. It does not need a lens to concentrate the light intensity on the receiver for increasing the current. Although we can use the photovoltaic cell (2CU33) as a photodetector, its rising edge time allows human eyes to perceive the LED flicker. Herein, we first build a transimpedance-operational amplifier to convert the current generated by the photodetector into a range of voltages. The output voltage is defined as

$$\begin{aligned}\text{Voltage (V)} = {} & \text{resposivity (A/W)} \times \text{optical power (W)} \\ & \times \text{transimpedance Gain (V/A)} \\ & \times \text{Scale Factor},\end{aligned} \tag{6}$$

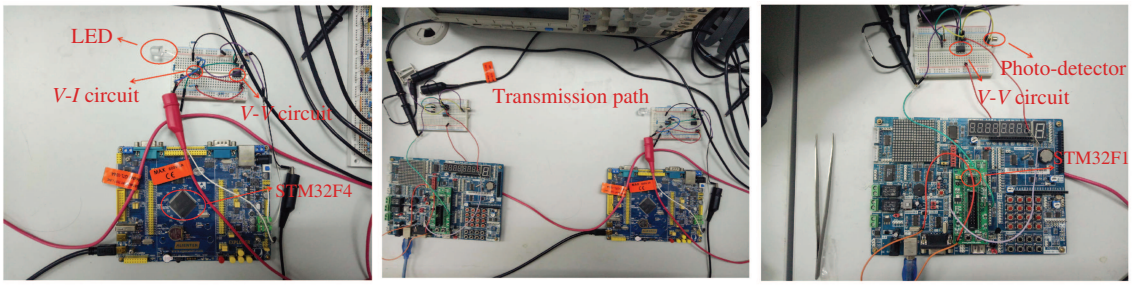

(a) (b) (c)

Figure 7 (Color online) The LED is operated by an STM32F407ZGT6 microcontroller and a V-I conversion circuit. The light intensity is converted into a voltage signal by the SD5412 photodetector. The voltage signal is sampled by the STM32F103C8 microcontroller. (a) The transmitter module; (b) transmission path; (c) the receiver module.

Table 2 Experimental parameters

System modules	
TX microcontroller	STM32F407ZGT6
TX voltage-to-voltage amplifier	LM358A
TX voltage-to-current amplifier	OPA07CPA
Transistor	S8050
RX voltage-to-voltage amplifier	LM358A
RX microcontroller	STM32F103C8
Power	GPS-430C
LED	SSL-LX100133XUWC
Photodetector	SD5412
TX characteristics	
Average optical power per LED	0.1 W
LED's FoV	120°
RX characteristics	
Photodetector diameter	2.54 mm
Receiver's FoV	120°
Photodetector responsivity R	0.87 (A/W)

$$\text{Scale Factor} = \frac{R_{\text{load}}}{R_{\text{load}} + 50\ \Omega}. \tag{7}$$

We find that the transimpedance-operational amplifier outputs 0–1.8 V when we test our experimental platform in all kinds of environments. Thus, we design a double closed-loop gain-operational amplifier circuit. This allows the STM32 to sample and investigate different voltage values. Meanwhile, it also protects the pins of the microcontroller, since 5 V is the maximum voltage for the input of the pin.

5 Evaluation

We conduct extensive experiments to evaluate the performance of our system in the following respects. (1) User perception: whether participants can perceive the LED flicker. (2) BER: we observe the BER of system with changing speeds and distances. (3) Other performances: we observe the system performance using the photovoltaic cell. Figure 7 shows and illustrates our experiment platform.

We conduct experiments in a typical office, where sunlight and fluorescent lights are present. Our main equipments are STM32F407ZGT6 microcontroller, voltage-to-current-converter circuit, voltage-to-voltage-amplifier circuit, SD5412 photodetector, and STM32F103C8 microcontroller. Specific device parameters and characteristics are listed in Table 2. We put the transmitter and receiver on the same horizontal line, and adjust the receiving light intensity by changing the distance between the transmitter and receiver. We use the constant-direct-current source GPS-430C to provide the power for operational

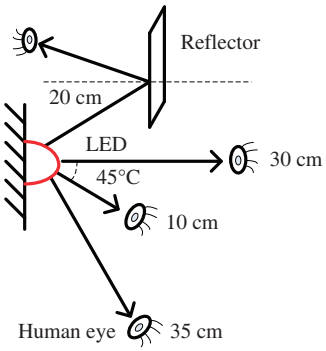

Figure 8 (Color online) User perception at different viewing angles. We list four different scenarios to observe whether the LED flicker impacts upon human eyes.

Table 3 User perception about the flicker

View	Speed (kbps)	Day flicker (%)	Night flicker (%)
Direct 30 cm	1	100	90
	3.3	0	25
	8	0	0
Indirect 10 cm	1	75	95
	3.3	5	5
	8	0	0
Indirect 35 cm	1	75	90
	3.3	0	25
	8	25	0
Reflect 20 cm	1	100	100
	3.3	0	5
	8	0	0

amplifier circuits. The laptop's USB Port provides power and serial communications. Eventually, we show two bit streams on the laptop screen.

5.1 User perception

We use the MAPPM scheme to transmit two bit streams. We recruit a total number of 20 men and women with ages between 18 and 50 to perform the human-eye-perception experiment. We consider four kinds of angle scenarios, as shown in Figure 8. (1) Direct viewing, where the participant stares directly into the LED and reports whether the LED is flickering. The distance between human eyes and the LED is 30 cm. (2) Indirect viewing at 35 cm. The distance between human eyes and the LED is 35 cm, the angle between human eyes and the LED is 70°. Human eyes observe the LED in this case. (3) Indirect viewing at 10 cm. The distance is 10 cm, the angle is 45°. (4) Reflected viewing at 20 cm. We use a piece of white paper to reflect the LED's light. The distance between human eyes and white paper is 40 cm and the distance between white paper and the LED is 20 cm. Human eyes detect whether the light from reflected paper appears to flicker. In each scenario, we further observe that human eyes perceive LED flicker at different speeds.

Table 3 lists participants' perception of flicker under several scenarios. Please note that we make use of the percentage to describe the average flicker perception of participants. If all participants agree that the LED is flickering, we will use 100%. If no one believes that the LED is flickering, we will use 0%. Through Table 3, we find that, when the speed is 1 kbps during both day and night, human eyes can detect flicker at all angles. This means that our system cannot use this speed for the data transmission. When the speed is 3.3 kbps, we do not perceive LED flicker in most situations. In particular, some participants could detect flicker when the distance was 35 cm or less between human eyes and the LED.

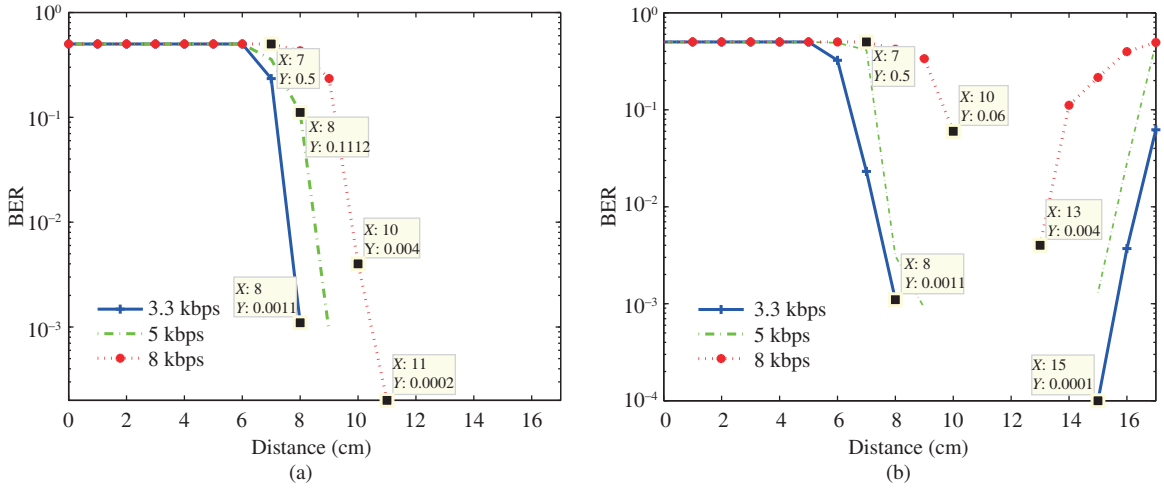

Figure 9 (Color online) The BER curve for the MAPPM scheme with Bits-1 (a) and Bits-2 (b) using different speeds and the receiver being located at different distances.

Furthermore, when we increase the speed to 8 kbps, most participants do not perceive the LED flicker in most situations. Therefore, we believe that the proposed MAPPM scheme is able to achieve the nonflicker requirement.

The flicker reason generated by the 1 kbps speed, we are not involved too much. The perception of flicker is related to human eyes' mesopic vision, Weber's law, ambient-light conditions, LED-color temperature, and other comprehensive factors [62–64]. In [64], the authors measured the ability of human eyes to perceive changes in brightness by conducting a large number of experiments in a scotopic-vision environment; they indirectly concluded that the current change at the μA level will not be perceived by human eyes when energy is supplied to the LED with a constant current source. For our experiments, since the transmitter and receiver exist in mesopic-vision environments and the Commission Internationale de I'Eclairage (CIE) has not yet given a specific mathematical model of mesopic vision, we make corresponding judgments only through actual perceptions.

While conducting experiments, we need to consider distances, responsivity of the photodiode, ambient-light interference, and other factors. Herein, we set the amplitude change of the transmitter port to 40 mv and the change in current to 100 μA by the converted resistance R_5. Please note that our experimental results differ from those of [64]. The main reason is that human eyes exist in various brightness environments, causing different proportions of rod and cone cells to work therein; therefore, the ability to perceive changes in brightness is not the same.

5.2 Bit-error rate

Now, we test the BER of the MAPPM scheme. We evaluate the impact of distances and speeds upon the BER. We make the LED transmit the synthetic bit stream 2000 times, each of which is picked up by the receiver. We transmit the pseudorandom sequence of 400 bits as a synthetic bit stream while using linear block codes as forward error-correction coding. The number of low levels is equal to that of high levels but the positions of these levels are random in each bit stream. Then, we collect the number of error bits during 2000 transmissions to calculate the BER. Our experimental results are shown in Figure 9.

In Figure 9(a), we plot the BER curve of Bits-1. The transmission speeds are 3.3, 5, and 8 kbps. In Figure 9(a), we find that the BER is high for 1–6 cm, reaching around 0.5. This is because SD5412 saturates, meaning that its output is a constant high level and the original low level is taken as the high level. As the distance increases, the BER drops to zero. For different speeds, the saturation distance generated by the photodetector differs. The speed is faster, the brightness is greater, and the saturation distance is longer.

In Figure 9(b), we plot the BER curve of Bits-2. Speeds and distances are the same as for Bits-1.

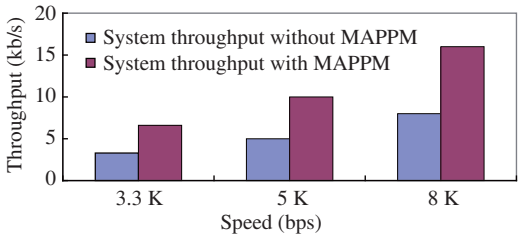

Figure 10 (Color online) The system throughput doubles at different speeds at a distance of 12 cm.

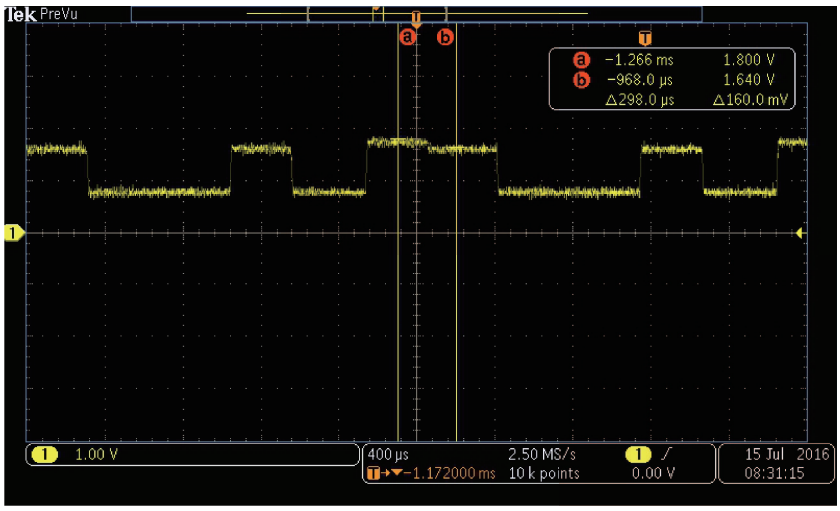

Figure 11 (Color online) The receiving waveform of the photodetector and V-V circuit under the interference condition at a distance of 15 cm.

Similarly, the BER is around 0.5 at a distance of 1–6 cm. This is because of saturation of the photodetector. As the distance increases, the BER drops to zero. When the distance is greater than 13 cm, the BER begins to increase again owing to a decrease in the brightness received by the photodetector with an increase in the distance. The photodetector does not identify the difference between the "softly bright" and "bright" levels. Meanwhile, under certain distance conditions, the increase of speed causes the BER to increase. The reason is that the receiver needs a certain time to respond. Rising and falling edges of the receiver produce "tailing" phenomena. The receiver needs to have a high-precision timer and A/D-converter module to judge and sample the data. When the sampling occurs at rising or falling edges, the BER will be generated.

Spectrum efficiency. For the spectrum efficiency, when distances and speeds are adjusted appropriately, we find that one symbol can represent two bits and the spectrum efficiency doubles. Furthermore, the system throughput is related to the spectrum efficiency. When this efficiency doubles, the system throughput doubles as well, as shown in Figure 10.

The initial experimental results demonstrate the feasibility of our framework. In this subsection, we further test the system's other performances by adding light interference, increasing communication distances, and using a photovoltaic cell. We discuss their impact in the following.

5.3 Adding light interference

For our current experiments, we use the SD5412 photodetector as the receiving end. We artificially add light noise to observe the receiver BER. We use the flashlight function of a mobile phone to generate light interference. We place the flashlight at the oblique top of the photodetector at 45° and at a distance of 8 cm. Figure 11 shows the output waveform of a photodetector under the interference condition at a distance of 15 cm. The waveform is very easily captured and recognized by the receiver because of the obvious difference between "bright" and "softly bright" light. The main form of interference is the

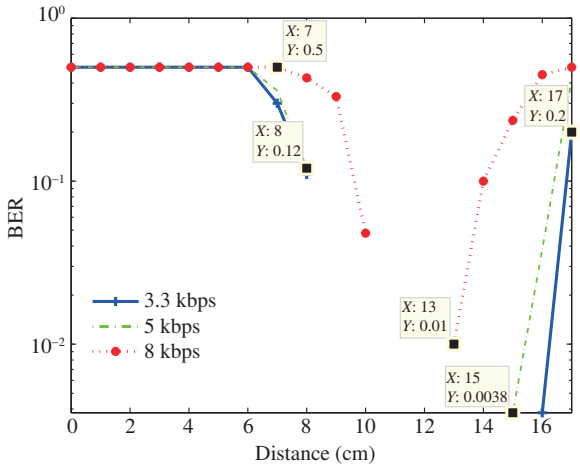

Figure 12 (Color online) The BER curve of Bits-2 under light interference.

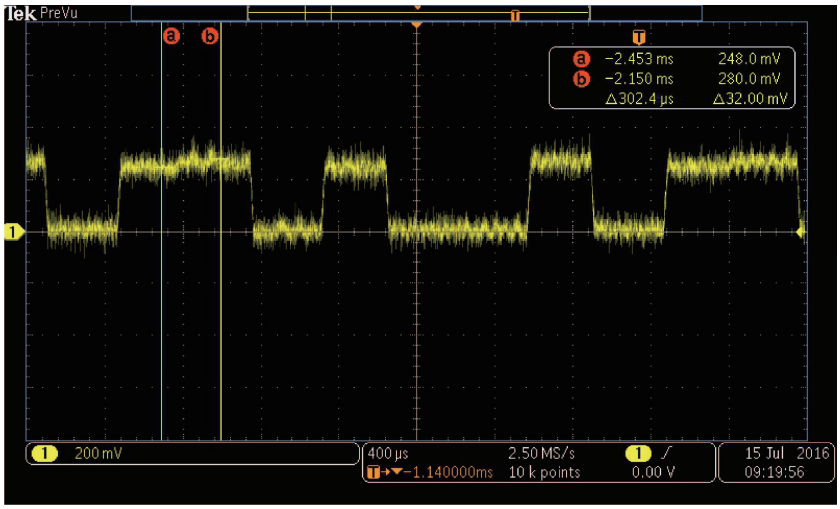

Figure 13 (Color online) The receiving waveform when the transmitter has six LEDs at a distance of 80 cm.

DC bias, with low- and high-level increase at the same time. This has no impact upon differentiating "bright" and "softly bright".

Figure 12 is the BER curve of Bits-2 under light interference. We do not show the BER curve of Bits-1, as there is a clear difference between the high and low levels for Bits-1. We do not repeat it here. In Figure 12, we find that Bits-2 is not affected by light interference. The overall BER of Bits-2 is the same as that in Figure 9(b). This is consistent with the results observed from the oscilloscope in Figure 11.

5.4 Communication distances

Herein, we evaluate the impact of the number of LEDs and the operational amplifier circuit closed-loop gain upon communication distances. We try to increase the number of LEDs and operational amplifier circuit's closed-loop gain for increasing communication distances. However, actual testing shows that these methods are not feasible.

Output waveform. We increase the transmitted light intensity by six series or parallel LEDs for increasing communication distances. Although this method increases the distance, the receiver cannot readily distinguish the square wave, as shown in Figure 13. The distance between the transmitter and receiver is 80 cm in Figure 13. There is no obvious difference between "bright" and "softly bright". The reason for this is that, (1) with an increase in the communication distances, light interference in environments will have a certain influence upon the receiver; (2) each LED differs from the others, making

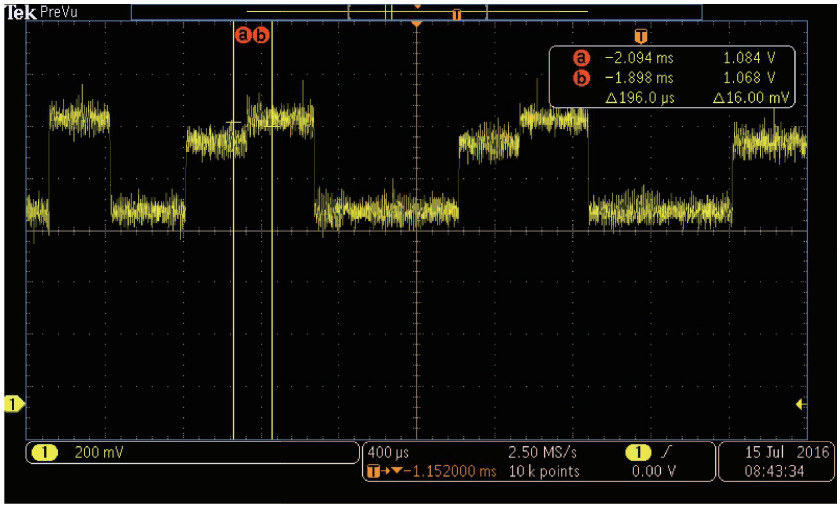

Figure 14 (Color online) The receiving waveform when the transmitter has six LEDs at a distance of 80 cm. Meanwhile, the closed-loop gain is 5.

it impossible to transmit the same light intensity. "Softly bright" and "bright" produce a superimposed light intensity upon each other and the final receiver cannot distinguish them.

We further distinguish "softly bright" and "bright" by increasing the closed-loop gain of the receiver's operational amplifier circuit so that it can sample and judge. We increase the closed-loop gain to 5, and the receiving waveform is shown in Figure 14. It can be seen that the main problem is that light noise is also amplified. Although we enlarge the charge of light intensity, we enlarge the noise caused by the transmitter's unstable electric level and ambient light at the same time. This has a significant impact on A/D conversion and threshold decision-making. For example, the a level should be lower than b in Figure 14 but it is not.

BER vs. distances. We present the BER curve of Bits-2 in the case of six LEDs, as shown in Figure 15. The communication distance increases to 80 cm and the whole curve is divided into three parts. When the communication distance ranges from 0 to 20 cm, the BER is high, reaching around 0.5. This is because the light emitted by the LED is too strong, causing the receiver's photodetector to become saturated; thus, it cannot distinguish between high and low levels. When the communication distance ranges from 20 to 60 cm, the BER decreases. When we increase the communication distance above 60 cm, the BER increases again. The major reason is that, when the communication distance increases, light noises have a certain effect upon the photodetector and the receiver cannot distinguish high from low levels. This result is consistent with Figure 13.

We also present the BER curve of Bits-2 in the case of 5 closed-loop gain, as shown in Figure 16. The BER is almost the same as that in Figure 15, except that when the communication distance ranges from 20 to 60 cm, the BER decreases. The reason for this decrease is that the 5 closed-loop high gain enables the receiver to distinguish Bits-2's high and low levels. However, the receiver still has judgment error under light noise. This is consistent with results observed in Figure 14.

5.5 Using a photovoltaic cell

Responsivity of the PV cell. We replace the SD5412 with a photovoltaic (PV) cell for receiving the synthetic bit stream. PV cells are more common and can also serve as storage for energy harvesting. However, we need to pay attention to the spectrum responsivity of the PV cell. The specific equation is as follows:

$$R_f = \frac{i_f}{P}, \tag{8}$$

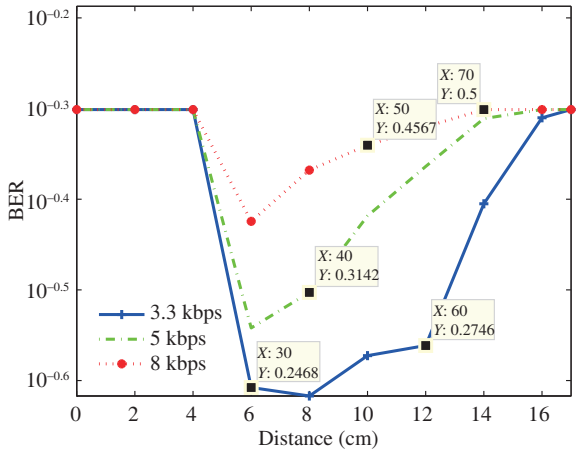

Figure 15 (Color online) The BER curve of Bits-2 in the case of six LEDs.

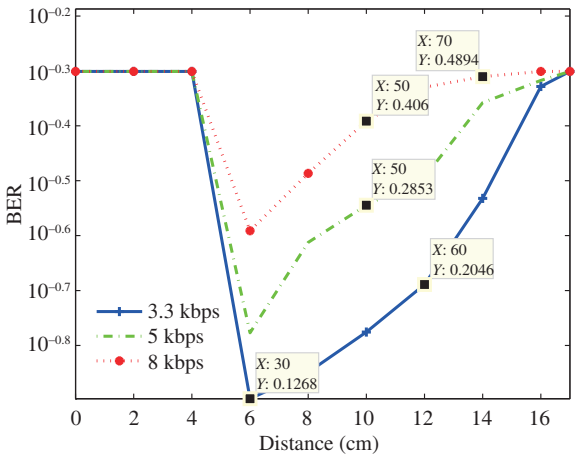

Figure 16 (Color online) The BER curve of Bits-2 in the case of 5 closed-loop gain.

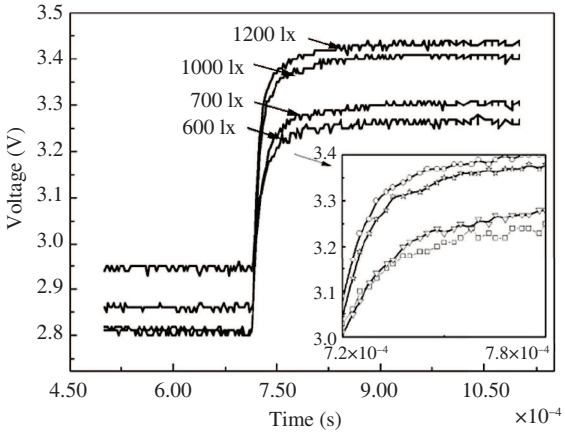

Figure 17 The curve of the PV cell-response time. We test response time and output voltage under different light intensities. The test data are transmitted at 1 KHz. Note that an enlarged view is given to the rising edge.

where R_f is the spectrum responsivity, P is the incident-light power, i_f is the Fourier transform value of the light-current time-varying function, generally defined as

$$i_f = \frac{i}{\sqrt{1 + (2\pi f \tau_c)}}, \tag{9}$$

where τ_c is the response time of the detector, which is decided by materials, structures, and external circuits.

We test the spectrum responsivity of the Si photovoltaic cell under different light intensities. The test data are 1 kHz and "dark, softly bright, bright" occurs in cycle. Results are shown in Figure 17. We find that the data from low level to stable high level need 60 μs, i.e., the rising edges need 60 μs. This means that one bit is actually transmitted by the 60 μs rising edge, 210 μs level, and 60μs falling edge. Such speed allows reception and judgment to take place but flicker will be perceived. We improve the frequency to 3.3 kHz. One bit needs 100 μs to finish the transmission. However, the rising and falling edges each take more than 60 μs. Thus, it does not generate the actual square waveform in this situation.

BER under the PV cell. We present the BER curve of Bits-1 and Bits-2 at 3.3 and 0.5 kbps, respectively, in the case of the PV cell. Through Figure 18, we can observe that the BERs of two bit streams are around 0.5 at 3.3 kbps. This is mainly because the PV cell's response time is not fast enough; therefore, the receiver samples signals at the rising or falling edges. This will generate random judgments on the receiver, resulting in varying BER. Thus, we can observe that the BER of the two bit streams is around 0 at 0.5 kbps, when the distance is between 5 and 10 cm. BER is around 0.2 at short distances,

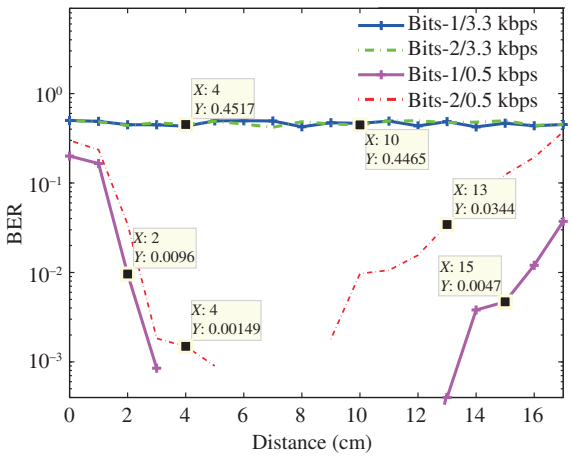

Figure 18 (Color online) The BER curve of two bit streams at 3.3 and 0.5 kbps when the PV cell is used as a photodetector.

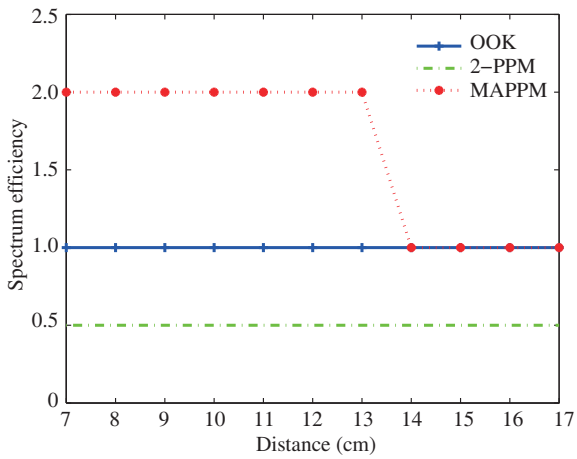

Figure 19 (Color online) We compare the spectrum efficiency of MAPPM with the OOK and 2-PPM methods and present the tradeoff relationship between spectrum efficiency and distance.

owing to PV cell saturation. Although the PV cell can achieve communication at 0.5 kbps, human eyes can perceive flicker.

5.6 Comparison with OOK and 2-PPM

We compared the proposed MAPPM with the OOK and 2-PPM methods and present the tradeoff relations between spectrum efficiency and distance, as shown in Figure 19. We set the length of a one-unit bit to be the same under the three modulation methods, and the transmission distance is set to 7–17 cm. When the transmission distance is less than 7 cm, no method is able to demodulate signals due to receiver's photodetector saturation. We use the spectrum efficiency of OOK modulation as the baseline for comparisons and we define it as 1. 2-PPM uses the lengths of two unit bits to represent one bit information; its spectral efficiency is half that of the OOK method. For our MAPPM, when the distance is 7–14 cm, the error rate is 0. Meanwhile, its spectrum efficiency is twice that of the OOK method. When the transmission distance increases, the sequence of Bits-2 will submerge in the light noise and our MAPPM can only decode the Bits-1 sequence. In this case, the spectrum efficiency of our MAPPM is the same as that of the OOK modulation method.

6 Conclusion

Herein, we have proposed a spectrum-efficient, low-complexity VLC system for indoor IoT applications. The key idea is to change the LED light intensity subtly to modulate two bit streams simultaneously while ensuring the photodetector is able to respond. In addition, we have further designed and implemented a voltage-to-current-amplifier circuit to mitigate the impact of the LED's flicker upon human eyes. Finally, we have prototyped the whole system using low-cost off-the-shelf devices, and evaluated it via thorough experiments. The experimental results have shown that our proposed approach is effective for improving the spectrum efficiency of low-complexity VLC systems with a very low cost.

Acknowledgements This work was supported in part by National Nature Science Foundation of China (Grant Nos. 61801105, 61501104, 61775033, 61771120), and in part by Fundamental Research Funds for the Central Universities (Grant Nos. N161604004, N161608001, N171602002).

References

1 Komine T, Nakagawa M. Fundamental analysis for visible-light communication system using LED lights. IEEE Trans Consumer Electron, 2004, 50: 100–107

2 Ibrahim M, Nguyen V, Rupavatharam S, et al. Visible light based activity sensing using ceiling photosensors. In: Proceedings of the Workshop on Visible Light Communication Systems, 2016. 43–48
3 Quintana C, Guerra V, Rufo J, et al. Reading lamp-based visible light communication system for in-flight entertainment. IEEE Trans Consumer Electron, 2013, 59: 31–37
4 Schmid S, Ziegler J, Corbellini G, et al. Using consumer led light bulbs for low-cost visible light communication systems. In: Proceedings of the Workshop on Visible Light Communication System, 2014
5 Xu J, Yao J M, Wang L, et al. Narrowband Internet of things: evolutions, technologies, and open issues. IEEE Internet Things J, 2018, 5: 1449–1462
6 Tian Z, Wright K, Zhou X. Lighting up the Internet of things with darkVLC. In: Proceedings of the 17th International Workshop on Mobile Computing Systems and Applications, 2016. 33–38
7 Schmid S, Corbellini G, Mangold S, et al. LED-to-LED visible light communication networks. In: Proceedings of the 14th ACM International Symposium on Mobile ad Hoc Networking and Computing, 2013. 1–10
8 Khalid A M, Cossu G, Corsini R, et al. 1-Gb/s transmission over a phosphorescent white LED by using rate-adaptive discrete multitone modulation. IEEE Photonic J, 2012, 4: 1465–1473
9 Tsonev D, Chun H, Rajbhandari S, et al. A 3-Gb/s single-LED OFDM-based wireless VLC link using a gallium nitride μ LED. IEEE Photon Technol Lett, 2014, 26: 637–640
10 Zhao L X, Zhu S C, Wu C H, et al. GaN-based LEDs for light communication. Sci China-Phys Mech Astron, 2016, 59: 107301
11 Singh R, O'Farrell T, David J P R. Performance evaluation of IEEE 802.15.7 CSK physical layer. In: Proceedings of IEEE Globlecom Workshops (GC Wkshps), Atlanta, 2013
12 Qian H, Cai S Z, Yao S J, et al. On the benefit of DMT modulation in nonlinear VLC systems. Opt Express, 2015, 23: 2618
13 Alaka S P, Narasimhan T L, Chockalingam A. On the performance of single- and multi-carrier modulation schemes for indoor visible light communication systems. In: Proceedings of IEEE Globecom, 2015
14 Wu F M, Lin C T, Wei C C, et al. Performance comparison of OFDM signal and CAP signal over high capacity RGB-LED-Based WDM visible light communication. IEEE Photonic J, 2013, 5: 7901507
15 Le N T, Nguyen T, Jang Y M. Frequency shift on-off keying for optical camera communication. In: Proceedings of the 6th International Conference on Ubiquitous and Future Networks (ICUFN), Shanghai, 2014
16 Popoola W, Poves E, Haas H. Generalised space shift keying for visible light communications. In: Proceedings of International Symposium on Communication Systems Networks Digital Signal Processing, 2012
17 Ghassemlooy Z, Popoola W, Rajbhandari S. Optical Wireless Communications: System and Channel Modelling with MATLAB. Abingdon: Taylor and Francis, 2012
18 Zeng Y, Green R J, Sun S B, et al. Tunable pulse amplitude and position modulation technique for reliable optical wireless communication channels. J Commun, 2007, 2: 22–28
19 Geng L, Wei J L, Penty R V, et al. 3 Gbit/s LED-based step index plastic optical fiber link using multilevel pulse amplitude modulation. In: Proceedings of Optical Fiber Communication Conference and Exposition and the National Fiber Optic Engineers Conference (OFC/NFOEC), Anaheim, 2013
20 Li H L, Chen X B, Huang B J, et al. High bandwidth visible light communications based on a post-equalization circuit. IEEE Photonic Tech Lett, 2014, 26: 119–122
21 Mirvakili A, Koomson V J. A flicker-free CMOS LED driver control circuit for visible light communication enabling concurrent data transmission and dimming control. Analog Integr Circ Sig Process, 2014, 80: 283–292
22 Park S B, Jung D K, Shin H S, et al. Information broadcasting system based on visible light signboard. In: Proceedings of Acta Press, 2007
23 Komine T, Lee J H, Haruyama S, et al. Adaptive equalization system for visible light wireless communication utilizing multiple white LED lighting equipment. IEEE Trans Wirel Commun, 2009, 8: 2892–2900
24 Galal M M, El Aziz A A, Fayed H A, et al. High speed data transmission over a visible light link employing smartphones xenon flashlight as a replacement of magnetic cards. In: Proceedings of IEEE High Capacity Optical Networks and Emerging/Enabling Technologies, 2013
25 Wu S, Wang H, Youn C H. Visible light communications for 5G wireless networking systems: from fixed to mobile communications. IEEE Netw, 2014, 28: 41–45
26 Park I H, Kim Y H, Jin Y K. Interference mitigation scheme of visible light communication systems for aircraft wireless applications. In: Proceedings of IEEE International Conference on Consumer Electronics (ICCE), Las Vegas, 2012
27 Haas H. Light fidelity (Li-Fi): towards all-optical networking. In: Proceedings of SPIE–The International Society for Optical Engineering, 2013. 900702
28 Kong L, Shen H, Xu W, et al. Transmission capacity maximization for LED array-assisted multiuser VLC systems. Sci China Inf Sci, 2015, 58: 082310
29 Biagi M, Vegni A M. Enabling high data rate VLC via MIMO-LEDs PPM. In: Proceedings of IEEE Globecom Workshops (GC Wkshps), Atlanta, 2013
30 Sugiyama H, Haruyama S, Nakagawa M. Brightness control methods for illumination and visible-light communication systems. In: Proceedings of ACM ICWMC, 2007
31 Lee K, Park H. Modulations for visible light communications with dimming control. IEEE Photonnic Technol Lett, 2011, 23: 1136–1138
32 Lin W Y, Chen C Y, Lu H H, et al. 10 m/500 Mbps WDM visible light communication systems. Opt Express, 2012, 20: 9919

33 Zhang Y Y, Yu H Y, Zhang J K. Block precoding for peak-limited MISO broadcast VLC: constellation-optimal structure and addition-unique designs. IEEE J Sel Areas Commun, 2018, 36: 78–90
34 Zhang Y Y, Yu H Y, Zhang J K, et al. Energy-efficient space-time modulation for indoor MISO visible light communications. Opt Lett, 2016, 41: 329
35 Chau J C, Morales C, Little T D C. Using spatial light modulators in MIMO visible light communication receivers to dynamically control the optical channel. In: Proceedings of the 2016 International Conference on Embedded Wireless Systems and Networks, Graz, 2016. 347–352
36 Gancarz J E, Elgala H, Little T D. Overlapping PPM for band-limited visible light communication and dimming. J Sol State Light, 2015, 2: 3
37 Tian Z, Wright K, Zhou X. The darklight rises: visible light communication in the dark. In: Proceedings of ACM Mobicom, 2016
38 Schmid S, Richner T, Mangold S, et al. Enlighting: an indoor visible light communication system based on networked light bulbs. In: Proceedings of 13th Annual IEEE International Conference on Sensing, Communication, and Networking (SECON), London, 2016
39 Narendran N, Gu Y M. Life of LED-based white light sources. J Display Technol, 2005, 1: 167–171
40 Pimputkar S, Speck J S, DenBaars S P, et al. Prospects for LED lighting. Nat Photonic, 2009, 3: 180–182
41 Lin H N. Low power consumption LED emergency light. US patent, EP2023033A1 F21L4/04, 2009
42 Bullough J D, Yuan Z, Rea M S. Perceived brightness of incandescent and LED aviation signal lights. Aviat Space Environ Med, 2007, 78: 893–900
43 Tang Y Y, Chen Q, Ju P, et al. Research on load characteristics of energy-saving lamp and LED lamp. In: Proceedings of IEEE Powercon, 2016
44 Prince G B, Little T D C. On the performance gains of cooperative transmission concepts in intensity modulated direct detection visible light communication networks. In: Proceedings of IEEE International Conference on Wireless and Mobile Communications, 2010
45 Yasir M, Ho S W, Vellambi B N. Indoor positioning system using visible light and accelerometer. J Lightw Technol, 2014, 32: 3306–3316
46 Li L Q, Hu P, Peng C Y, et al. Epsilon: a visible light based positioning system. In: Proceedings of ACM/USENIX NSDI, 2014
47 Hu P, Li L Q, Peng C Y, et al. Pharos: enable physical analytics through visible light based indoor localization. In: Proceedings of ACM HotNets-XII, 2014
48 Arai S, Mase S, Yamazato T, et al. Experimental on hierarchical transmission scheme for visible light communication using LED traffic light and high-speed camera. In: Proceedings of IEEE 66th Vehicular Technology Conference, 2007
49 Wang Q, Giustiniano D, Puccinelli D. Openvlc: software-defined visible light embedded networks. In: Proceedings of ACM Mobicom, 2014
50 Li T X, An C K, Xiao X R, et al. Real-time screen-camera communication behind any scene. In: Proceedings of ACM MobiSys, 2015
51 Hao T, Zhou R G, Xing G L. Cobra: color barcode streaming for smartphone systems. In: Proceedings of ACM MobiSys, 2012
52 Wang A R, Peng C Y, Zhang O Y, et al. Inframe: multiflexing full-frame visible communication channel for humans and devices. In: Proceedings of ACM HotNets-XIII, 2014
53 Schmid S, Mangold S, Richner T, et al. Linux light bulbs: enabling internet protocol connectivity for light bulb networks. In: Proceedings of ACM VLCS, 2015
54 Schmid S, Corbellini G, Mangold S, et al. Continuous synchronization for LED-to-LED visible light communication networks. In: Proceedings of IEEE IWOW, 2014
55 Gupta S, Chen K Y, Reynolds M S, et al. Lightwave: using compact fluorescent lights as sensors. In: Proceedings of ACM UBICOMP, 2011. 65–74
56 Schmidt D, Molyneaux D, Cao X. Picontrol: using a handheld projector for direct control of physical devices through visible light. In: Proceedings of ACM UIST, 2012
57 Zhou X, Campbell A T. Visible light networking and sensing. In: Proceedings of ACM HotWireless, 2014
58 Stefan I, Burchardt H, Haas H. Area spectral efficiency performance comparison between VLC and RF femtocell networks. In: Proceedings of IEEE International Conference on Communications (ICC), 2013
59 IEEE Standards Association. 802.15.7-2011 - IEEE Standard for Local and Metropolitan Area Networks-Part 15.7: Short-Range Wireless Optical Communication Using Visible Light. 978-0-7381-6665-0. https://ieeexplore.ieee.org/servlet/opac?punumber =6016193
60 Stone P T. Review paper: fluorescent lighting and health. In: Proceedings of SAGE Lighting Research and Technology, 1992
61 Ndjiongue A R, Thokozani Shongwe, Ferreira H C, et al. Cascaded PLC-VLC channel using OFDM and CSK techniques. In: Proceedings of IEEE Globecom, 2015
62 Dabeer O, Chaudhuri S. Analysis of an adaptive sampler based on Weber's law. IEEE Trans Signal Process, 2011, 59: 1868–1878
63 Brown A M, Dobson V, Maier J. Visual acuity of human infants at scotopic, mesopic and photopic luminances. Vision Res, 1987, 27: 1845–1858
64 Jinno M, Morita K, Tomita Y, et al. Effective illuminance improvement of a light source by using pulse modulation and its psychophysical effect on the human eye. J Light Vis Env, 2008, 32: 161–169